Published online 4 June 2010

Nucleic Acids Research, 2010, Vol. 38, No. 19 ***6447–6455***
doi:10.1093/nar/gkq518

Divergent β-hairpins determine double-strand versus single-strand substrate recognition of human AlkB-homologues 2 and 3

Vivi Talstad Monsen[1], Ottar Sundheim[1], Per Arne Aas[1], Marianne P. Westbye[1], Mirta M. L. Sousa[1,2], Geir Slupphaug[1,2] and Hans E. Krokan[1,*]

[1]Department of Cancer Research and Molecular Medicine, Faculty of Medicine and [2]The FUGE Proteomics Laboratory, Norwegian University of Science and Technology, N-7489 Trondheim, Norway

Received March 10, 2010; Revised May 19, 2010; Accepted May 23, 2010

ABSTRACT

Human AlkB homologues ABH2 and ABH3 repair 1-methyladenine and 3-methylcytosine in DNA/RNA by oxidative demethylation. The enzymes have similar overall folds and active sites, but are functionally divergent. ABH2 efficiently demethylates both single- and double-stranded (ds) DNA, whereas ABH3 has a strong preference for single-stranded DNA and RNA. We find that divergent F1 β-hairpins in proximity of the active sites of ABH2 and ABH3 are central for substrate specificities. Swapping F1 hairpins between the enzymes resulted in hybrid proteins resembling the donor proteins. Surprisingly, mutation of the intercalating residue F102 had little effect on activity, while the double mutant V101A/F102A was catalytically impaired. These residues form part of an important hydrophobic network only present in ABH2. In this functionally important network, F124 stacks with the flipped out base while L157 apparently functions as a buffer stop to position the lesion in the catalytic pocket for repair. F1 in ABH3 contains charged and polar residues preventing use of dsDNA substrate. Thus, E123 in ABH3 corresponds to F102 in ABH2 and the E123F-variant gained capacity to repair dsDNA with no loss in single strand repair capacity. In conclusion, divergent sequences outside of the active site determine substrate specificities of ABH2 and ABH3.

INTRODUCTION

Cells are continuously exposed to agents that methylate DNA, such as tobacco-specific nitrosamines (1) and cellular *S*-adenosylmethionine (2). In addition, methylating drugs, e.g. temozolomide, are used in cancer treatment (3). Importantly, repair enzymes may modulate sensitivity to methylating agents. Among these are *Escherichia coli* AlkB and human AlkB homologues 2 and 3 (ABH2, ABH3) that directly repair 1-methyladenine (1-meA), 3-methylcytosine (3-meC) and some other base lesions in DNA, using ferrous iron and 2-oxoglutarate (2OG) for oxidative demethylation (4–7). The reactive iron is co-ordinated by a conserved HxD/Ex_NH motif in a double-stranded (ds) β-roll-fold as in other members of the dioxygenase superfamily (8). Their catalytic core domains have similar overall fold (9–12), but divergent flexible loop segments with distinct conformations are likely motifs important for substrate specificity in AlkB, ABH2 (11) and ABH3 (13).

ABH2 repairs methylations in dsDNA and single-stranded (ss) DNA. It is strictly nuclear and during S-phase it localizes in replication foci (7) where it interacts with proliferating cell nuclear antigen through the recently identified APIM-motif (14). Mouse knockout cells with targeted disruption in the *Abh2*-gene demonstrated reduced repair of 1-meA in DNA. They also displayed increased sensitivity to methylating agents and measurable accumulation of 1-meA in the genome even without exposure. In contrast, no indication of reduced repair was observed in ABH3 knockout cells (15). This indicates that ABH2 is a major demethylase, while the *in vivo* roles of ABH3 and other AlkB homologues remain obscure. ABH3 has a strong preference for ssDNA substrate, but also efficiently demethylates RNA (7,16). A likely function of ABH3 other than DNA repair is also indicated by its localization to nuclei and cytoplasm (7).

Given the high structural similarity of ABH2 and ABH3, their divergent functions would seem surprising. The crystal structures of ABH3 and ABH2 have given

*To whom correspondence should be addressed. Tel: +47 72 57 30 74; Fax: +47 72 57 64 00; Email: hans.krokan@ntnu.no

important insights into their biochemical mechanisms of action. However, for ABH2 no mutagenesis experiments to back up structural data are available and for ABH3, mutagenesis has mostly explored the function of active site residues. Short divergent β-hairpins (F1) in ABH2 and ABH3 in proximity of the active sites have been implicated in substrate binding from structural data (9,11).

Here, we have explored the function of the F1 loops and residues that interact with these loops in ABH2 and ABH3 (13). Motif swapping and site-directed mutagenesis reveal that the divergent F1 motifs in ABH2 and ABH3 are essential for substrate specificity of the enzymes. F1 of ABH2 intercalates into the dsDNA minor groove and F102 was suggested to aid flipping of the damaged base into the active site of ABH2 (11). Surprisingly, we find that F102 can be mutated to Ala with little consequence for ds or ssDNA repair, while the hydrophobic neighbour V101 is very important. Furthermore, the activity of the V101A/F102A double mutant is catalytically strongly impaired. In addition, V99 that interacts with both V101 and F102, is also important for demethylation of both ss and dsDNA. Moreover, we have identified a hydrophobic network extending beyond the F1 loop in ABH2. This network appears to be tailored to ensure proper substrate-binding, stable flipping and exact positioning of the damaged base in the active site.

MATERIALS AND METHODS

Site-directed mutagenesis and construction of hybrid and deletion proteins

Plasmids encoding ABH2 or ABH3 (7) were used to generate all mutant proteins. Site-directed mutagenesis was conducted according to the standard QuickChange protocol (Stratagene) and the entire coding sequence of the vector was sequenced to confirm the presence of the correct mutation. Identity of the F102A variant was additionally confirmed by MALDI time-of-flight mass spectrometry analyses of peptides after trypsin digestion.

ABH2-F1AB3 and ABH3-F1AB2 hybrid proteins were generated by switching amino acids V89 to V108 (F1) in ABH2 with V113 to Q129 (F1) in ABH3. To construct the ABH2-F1AB3 hybrid, the F1 insert fragment of ABH3 was amplified by PCR with Turbo Pfu DNA Polymerase (Stratagene), using ABH3 pET-28a plasmid and primers 1 and 2 (Supplementary Table S1). The entire ABH2 pET-28a plasmid with exception of the F1 fragment was amplified by PCR using primers 3 and 4 (Supplementary Table S1). PCR produced blunt end fragments that were purified from agarose gel (QIAquick gel extraction kit, Qiagen). The F1 containing insert fragment from ABH3 was placed into the ABH2 plasmid with the F1 containing segment deleted, using Quick Ligase (NEB) before cloning into DH5α cells. To construct the ABH3-F1AB2 hybrid, we used a strategy creating a mega-primer (17) sequentially used to produce the desired construct. More detailed, the F1 insert fragment of ABH2 was amplified by PCR using ABH2 pET-28a plasmid and primers 5 and 6 (Supplementary Table S1), producing a fragment of ABH2 containing F1 with flanking sequences from ABH3 wild-type (wt) protein. Two separate PCR reactions were next performed, both with the fragment produced in the previous step and ABH3 pET-28a plasmid. The first PCR included the T7 promotor primer and the second included the T7 terminator primer. The two fragments produced held ABH2 F1, the first also contained the sequence preceding F1 in ABH3 (from the T7 promotor primer site to D112) and the latter contained the sequence after F1 in ABH3 (from P130 to the end of the T7 terminator primer site). The two resulting fragments were purified from agarose gel and joined by PCR. Correct plasmid construction was verified by sequencing of the entire coding sequence and examining directionality of the insert by PCR and restriction enzyme digestion.

F1 deletion mutants ABH2Δ89-108 and ABH3Δ113-129 were generated by deleting amino acids V89 to V108 in ABH2 and V113 to Q129 in ABH3. The entire ABH2 or ABH3 pET-28a plasmid minus the segment to be deleted was amplified by PCR, producing blunt ended constructs purified by gel extraction, 5′-phosphorylated with T4 polynucleotide kinase (NEB) and ligated with Quick ligase (NEB). Deletions were verified by gel electrophoresis of digested plasmid products, in addition to sequencing of the entire coding sequence. Primer set 3/4 for ABH2Δ89-108 and primer set 9/10 for ABH3Δ113-129 were used to accomplish the deletion (Supplementary Table S1).

Expression and purification of ABH2 and ABH3

The wt and mutant proteins were expressed in *E. coli* BL21(DE3)RIPL cells grown at 37°C in Luria–Bertani medium with kanamycin (30 μg/ml). When OD_{600} reached 0.6, cultures were induced with isopropyl β-D-thiogalactoside (0.1 mM) for 4 h at 37°C before harvesting. Cells were re-suspended in a buffer of 50 mM Na_2PO_4 (pH 7.5), 300 mM NaCl, 0.01% Tween 20, 1× Complete-Protease inhibitor (EDTA-free, Roche), 2 mM β-mercaptoethanol and lysed by sonication. Mutant and wt proteins were purified as described (7), with some modifications. Immobilized metal affinity chromatography was used to purify cleared cell lysates (TALON resin, Clontech) and protein fractions were additionally purified by ion exchange chromatography, using a HiTrap SP HP sepharose column (GE Healthcare) and eluting with a NaCl gradient. Protein purity was verified by SDS–PAGE (Supplementary Figure S1) and concentrations determined using the Experion system (BioRad).

DNA repair assay

Repair of 3-meC in ss and dsDNA oligonucleotide substrates was determined as described (18), with some modifications. A carboxyfluorescein end-labelled 49-mer oligonucleotide (ss or dsDNA) containing 3-meC in the recognition site for the methylation-sensitive restriction endonuclease DpnII was used as substrate for purified AlkB homologues. The 3-meC oligonucleotides were incubated with enzyme and subsequently cut with DpnII. Generation of cleavable substrate was then

monitored after separation of fragments by denaturing PAGE. For single-turnover assays, ABH2 wt or amino acid variants (1 pmol) were incubated with ss or ds oligonucleotide substrate (1 pmol). To assay repair of ABH3 wt and amino acid variants, 1 pmol of oligonucleotide substrate was incubated with 10 pmol of enzyme. To further characterize the enzymatic activity of wt ABH2 and ABH3 and hybrid enzymes, increasing amounts of enzyme (0.3, 1, 3 and 10 pmol) were incubated with 1 pmol of ss or ds oligonucleotide substrate. All reactions were run at 37°C for 20 min in a 50 µl reaction mix and assays were run at least three times if not otherwise stated. Buffer composition was optimized for ABH2 and ABH3 wt and hybrid enzymes with ss and ds substrates (results not shown). Activity of all enzymes was assayed in a buffer of 200 µM 2OG, 20 µM $FeSO_4$ and 100 µg/ml BSA. For ABH2 enzyme and mutants assayed with ss substrate, the buffer contained additionally 20 mM Tris (pH 7.9), 200 mM KCl and 2 mM ascorbic acid. The same buffer with increased KCl concentration (300 mM) was used for ds substrate. For ABH2-F1AB3 the same buffer was used for both substrates and contained additionally 20 mM Tris (pH 7.9), 100 mM KCl and 2 mM ascorbic acid. For ABH3 enzyme, mutants and ABH3-F1AB2 the same buffer was used for both substrates and contained aditionally 20 mM Tris (pH 7.0), 80 mM KCl and 4 mM ascorbic acid. The ds oligo substrate was prepared by annealing 3× molar excess of complementary oligo to the 3-meC containing oligo in a buffer of 10 mM Tris pH 8.0 and 50 mM KCl.

CO_2 release assay for 2OG turnover

Deletion mutants were assayed for turnover activity of radioactively labelled 2OG as described earlier (18). In more detail, ABH2, ABH3, ABH2Δ89-108 and ABH3Δ113-129 were incubated with 100 µM 2OG containing 10% 1-[^{14}C]2OG (54.5 mCi/mmol specific activity) in a reaction buffer previously indicated. Hyamine hydroxide in a separate tube (2 M, 150 µl) was placed into each sample vial and the vials were closed. Reactions were incubated at 37°C for 1 h, quenched by addition of trifluoroacetic acid (50%, 15 µl) and further incubated on ice for 1 h. The release of $^{14}CO_2$ from 1-[^{14}C]2OG was detected by scintillation counting of the hyamine hydroxide solution.

Illustrations

Structural images were made in PyMOL, DeLano, W.L. The PyMOL Molecular Graphics System (2002) DeLano Scientific, Palo Alto, CA, USA (http://www.pymol.org), and figures prepared for publication using Adobe Illustrator CSIII (http://www.adobe.com/).

RESULTS

Divergent F1 loops in ABH2 and ABH3 are essential for demethylase activity and substrate specificity

The F1 loops in proximity of the active sites are composed of 20 and 17 residues in ABH2 and ABH3, respectively. In addition to a β-hairpin, ABH2 F1 contains a short α helix, forming an F1 loop equal in length to the one in ABH3 (Figure 1A). The primary structure of ABH2 F1 is hydrophobic, whereas ABH3 F1 has excess of charged and hydrophilic residues. Deleting the F1 loop (Figure 1B), creating ABH2Δ89-108 and ABH3Δ113-129, abolished repair activity for 3-meC in ss and dsDNA (data not shown). However, ABH2Δ89-108 retained ability to turn over 2OG to succinate and CO_2, indicating intact catalytic domain (Supplementary Figure S3). ABH2 is approximately equally active on ds and ssDNA, while ABH3 has at least 30-fold preference for ssDNA (Figure 1C and D). To examine the significance of the F1 loops for substrate specificity, we swapped these segments between ABH2 and ABH3 (Figure 1B). The resulting ABH3-F1AB2 hybrid repaired 3-meC in ssDNA with efficiency similar to wt ABH2 and ABH3 (Figure 1C). Furthermore, ABH3-F1AB2 had markedly increased ability to repair 3-meC in dsDNA, when compared with ABH3 (Figure 1D). In contrast, the opposite hybrid, ABH2-F1AB3 was catalytically dead with dsDNA, but displayed measurable demethylase activity on ssDNA, although strongly reduced compared with wt (Figure 1C and D).

These results demonstrate that the unique ability of ABH2 to efficiently repair 3-meC in dsDNA is specified mainly by the F1 hairpin. Similarly, the F1 hairpin of ABH3 mediates ssDNA substrate preference. Whereas the F1 hairpin deletion mutant ABH2Δ89-108 lost all demethylase activity, this protein retained ability to decarboxylate 2OG, indicating that the catalytic domain is intact. In contrast, deletion of F1 in ABH3 resulted in loss of both demethylase and decarboxylase activity, indicating a possible effect on the overall structure of the catalytic domain.

Acidic residues in ABH3 F1 discriminate against use of dsDNA substrate

ABH3-R122 and ABH3-E123 in the F1 β-hairpin have been implicated in substrate interaction (9). To explore substrate preferences further we generated ABH3 ss or ds mutants in which F1 residues R122, E123, D124 or Y127 were replaced by the structurally corresponding residues in ABH2 (13). Previously, we demonstrated that replacing the putative intercalating R122 by Ala (ABH3-R122A) reduced activity towards ssDNA moderately and dsDNA substrate strongly (9). In contrast, the R122V mutant had full activity with ssDNA and only very slightly reduced activity with dsDNA substrate (Figure 2A). Thus, a positive charge at residue 122 is not required for substrate discrimination. However, the length of the side chain of this residue is important both for activity and ds/ssDNA discrimination, indicating a possible finger–residue function of R122. Note that in the figure, activity with ss and dsDNA substrate has been normalized to 1, although absolute activity with ssDNA is >30-fold higher than with dsDNA. Single residue mutants ABH3-E123F and ABH3-D124G displayed 5.2- and 2.5-fold increased activity with dsDNA substrate, respectively. They are, however, not required

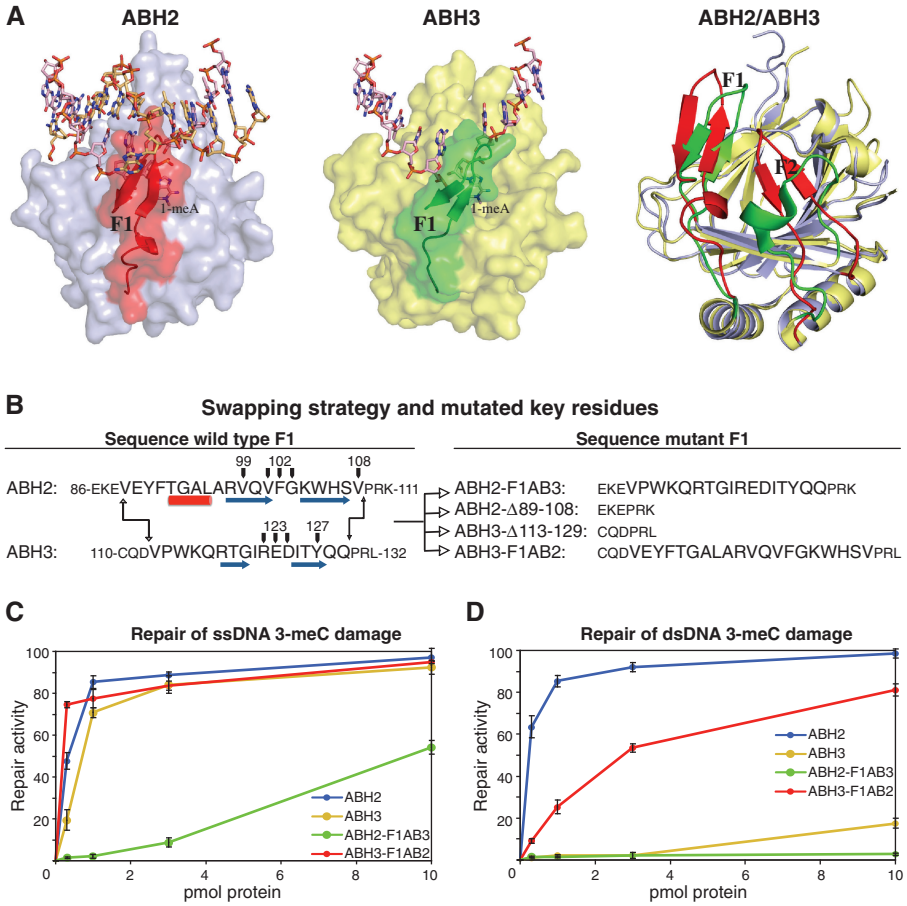

Figure 1. ABH2 and ABH3 structures, mutagenesis strategy and repair activity of hybrid proteins. (**A**) Left and middle: surface presentations of ABH2 (PDB ID: 3buc) and ABH3 (PDB ID: 2iuw) with bound ds and ssDNA substrate, respectively. The 1-meA in the active sites is indicated. The coordinates for the lesion-containing strand in ABH3 were obtained by superimposing the ABH3 (PDB ID 2iuw) onto cross-linked ABH2-dsDNA (PDB ID 3buc). The F1 motifs are shown as ribbons and highlighted in red and green for ABH2 and ABH3, respectively. Right: superimposed ABH2 (light blue) and ABH3 (light yellow) structures presented as ribbons with the DNA recognition lid coloured in red for ABH2 and green for ABH3. (**B**) Swapping strategy and key residues mutated. The α-helix (red cylinder) and β-strands (blue arrows) in F1 of ABH2 and ABH3 are indicated below the wt sequences. Residues in F1 selected for site directed mutagenesis are marked with black vertical arrows. (**C** and **D**) Repair activities of ABH2 and ABH3 wt and F1 hybrid proteins on ss (C) and ds (D) 3-meC DNA substrate. Each data point is the result of four independent experiments with standard deviation indicated as error bars.

for activity on ssDNA substrate, suggesting that the role of E123 and D124 is to prevent use of dsDNA substrate. Noticeably, the ABH3-E123F mutant displayed activity on dsDNA substrate approaching that of the ABH3-F1AB2 hybrid. Creating a local hydrophobic ABH2-like wedge at the tip of F1 β4-β5 in ABH3 (R122V/E123F) also markedly increased dsDNA activity, although not quite to the level of the E123F mutant. ABH3-Y127 points its phenolic hydroxyl into the putative DNA-binding groove (Figure 2B). A His residue is found in the equivalent position in ABH2. The ABH3-Y127H variant displayed wt activity on ssDNA substrate, and 1.4-fold increase in activity with dsDNA (Figure 2A). In conclusion, E123 and D124 are major determinants for the ssDNA specificity of ABH3 while Y127 has a more limited role.

Wedging dsDNA with F102 is dependent on V101 in ABH2

The side chain of F102 in ABH2 is inserted into the base stack of duplex DNA and occupies the vacant space resulting from base flipping, indicating a prominent role of this residue (11). Unexpectedly, the F102A variant retained 100 and 80% activity towards 3-meC in ssDNA and dsDNA, respectively. In contrast, the V101A variant retained only 40 and 20% demethylase activity on ss and dsDNA substrate, respectively. Furthermore, the double mutant V101A/F102A retained <10% of wt activity (Figure 3A), demonstrating the importance of this interacting hydrophobic pair in the F1 loop (Figure 3B). The significance of V101 was further investigated by introducing Gly and Ser in this position. Removing the side chain (ABH2-V101G) resulted in a protein with hardly detectable activity on dsDNA substrate and only 15% activity on ssDNA. However, when introducing the small polar serine (ABH2-V101S), almost 50% of the wt activity on ssDNA was retained, whereas activity with dsDNA substrate was very low. Similarly, the ABH2-V101R mutant had close to wt activity on ssDNA, but strongly impaired activity on dsDNA. All mutants displayed similar properties when assayed in 3 : 1 excess of protein compared with substrate, indicating

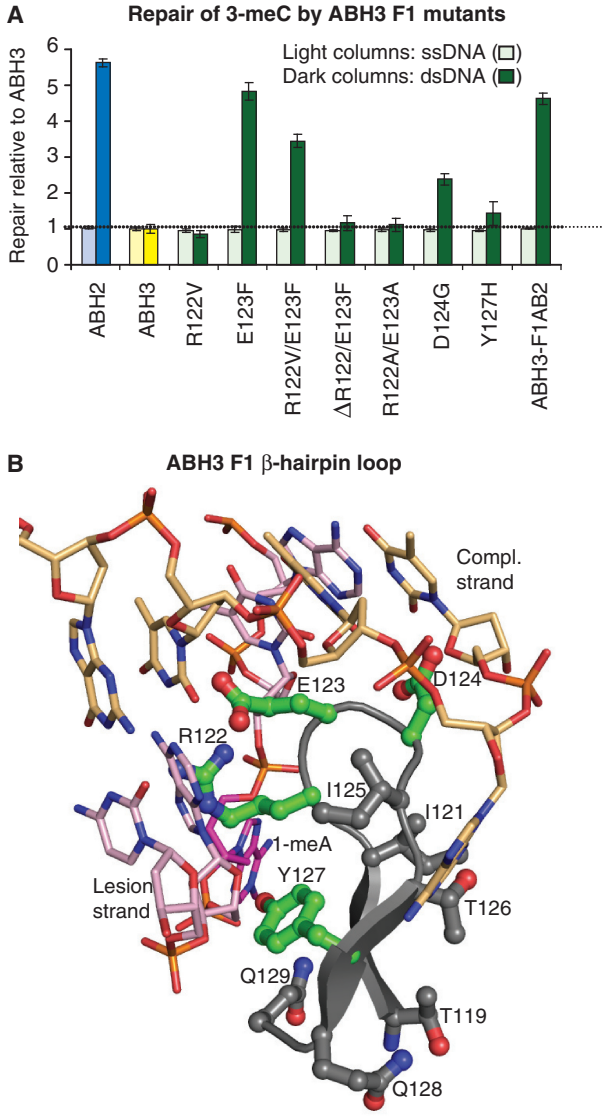

Figure 2. Substrate preference of ABH3 F1 mutants. (**A**) Repair activity of ABH3 F1 mutants and ABH2 relative to wtABH3. The 1 pmol substrate was incubated with 10 pmol protein for 20 min at 37°C. Repair of 3-meC in ss or dsDNA is presented relative to that of wtABH3, for which relative repair is normalized to a value of 1 for both ss and dsDNA repair. Results are from at least three independent experiments with standard deviation indicated. (**B**) Close-up view of ABH3 F1 β-hairpin residues (balls and sticks) (PDB ID: 2iuw). Residues selected for mutational studies are shown in green. The co-ordinates for the dsDNA (lines) were obtained after superimposing ABH3 onto ABH2. The 1-meA in extra-helical position is in magenta.

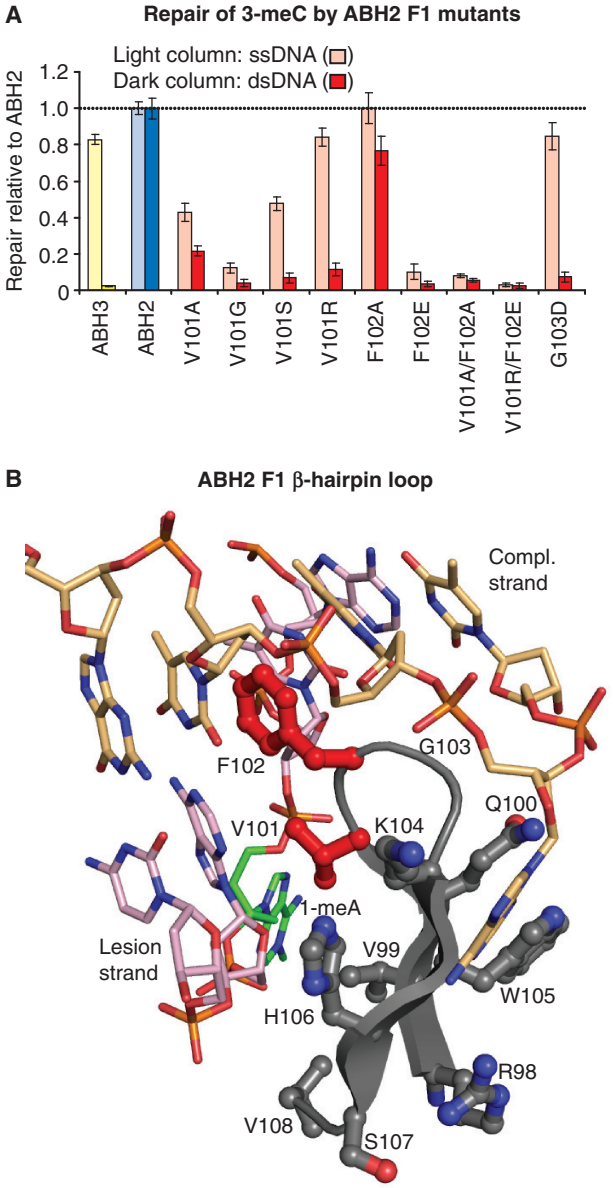

Figure 3. Repair activity of ABH2 and role of hydrophobic F1 wedge. (**A**) The 1 pmol substrate was incubated with 1 pmol protein for 20 min at 37°C. Columns display repair of 3-meC in ss or dsDNA by F1 wedge mutants, compared to wtABH2. Relative activities were normalized to wt ABH2 (set to 1) for repair of ss and dsDNA substrate. Repair was quantified from at least three independent experiments, with standard deviation indicated. (**B**) Close-up view of residues (balls and sticks) in the F1 β-hairpin motif in ABH2 (PDB ID: 3buc). Residues selected for mutagenesis are coloured red. Duplex DNA (lines) in pink and gold for lesion and complementary strand, respectively. The 1-meA in extra-helical position is in green.

that single turnover is also impaired (data not shown). G103 in ABH2 corresponds to D124 in ABH3; thus we generated an ABH2-G103D mutant to test if this ABH2-variant would also lose ABH2 properties and gain ABH3-like properties. Indeed, we observed a strong reduction in demethylase activity with dsDNA substrate, whereas activity with ssDNA was essentially retained (Figure 3A). The charged F1 residues R122 and E123 in ABH3 correspond to V101 and F102 in ABH2 structure. However, the catalytic efficiency of the ABH2-F102E mutant was <10% on both ss and dsDNA substrate, whereas the double mutant V101R/F102E was catalytically dead (Figure 3A).

These results demonstrate the significance of hydrophobic intercalating residues in F1 of ABH2 for activity on dsDNA. Substitution with charged and polar residues in the F1 β-hairpin compromises use of duplex DNA as substrate and results in an enzyme that gain ABH3-like properties.

ABH2 F1 is part of a functionally important hydrophobic network

The unexpected importance of ABH2-V101 prompted us to examine other conserved hydrophobic residues in F1 of ABH2. A hydrophobic network of interacting residues was found using the Protein Interactions Calculator web server, when setting a cut-off value at 5Å (19). Analysis of mutants demonstrated that most of these hydrophobic residues are indeed important for activity (Figure 4). Central in this network is V99 that interacts with V101 and V108 in F1 and F124 and L127 in F2 (defined in Figure 1). Substituting V99 or V108 with a smaller Ala residue reduced demethylase activity significantly, and the double Ala mutant rendered the enzyme essentially inactive (Figure 4C). Gly and Glu variants in position 99 and 108 also impaired activity of ABH2. Leu and Ile variants, present in some species (Supplementary Figure S4) were less affected (Figure 4C, and data not shown).

Introducing Thr in positions 99 or 108 would cause minor changes in occupied space compared to Val, but some hydrophobic interactions would be lost due to the hydroxyl group. Interestingly, the ABH2-V99T and V99A mutants displayed similar activity against ssDNA. However, V99T retained only ~30% activity against dsDNA substrate when compared to V99A. This may suggest that flipping of the damaged base in a dsDNA context is dependent of a cooperative interaction between the two strands of the intercalating β-hairpin loop. Introducing a hydroxyl group (in V108T) instead

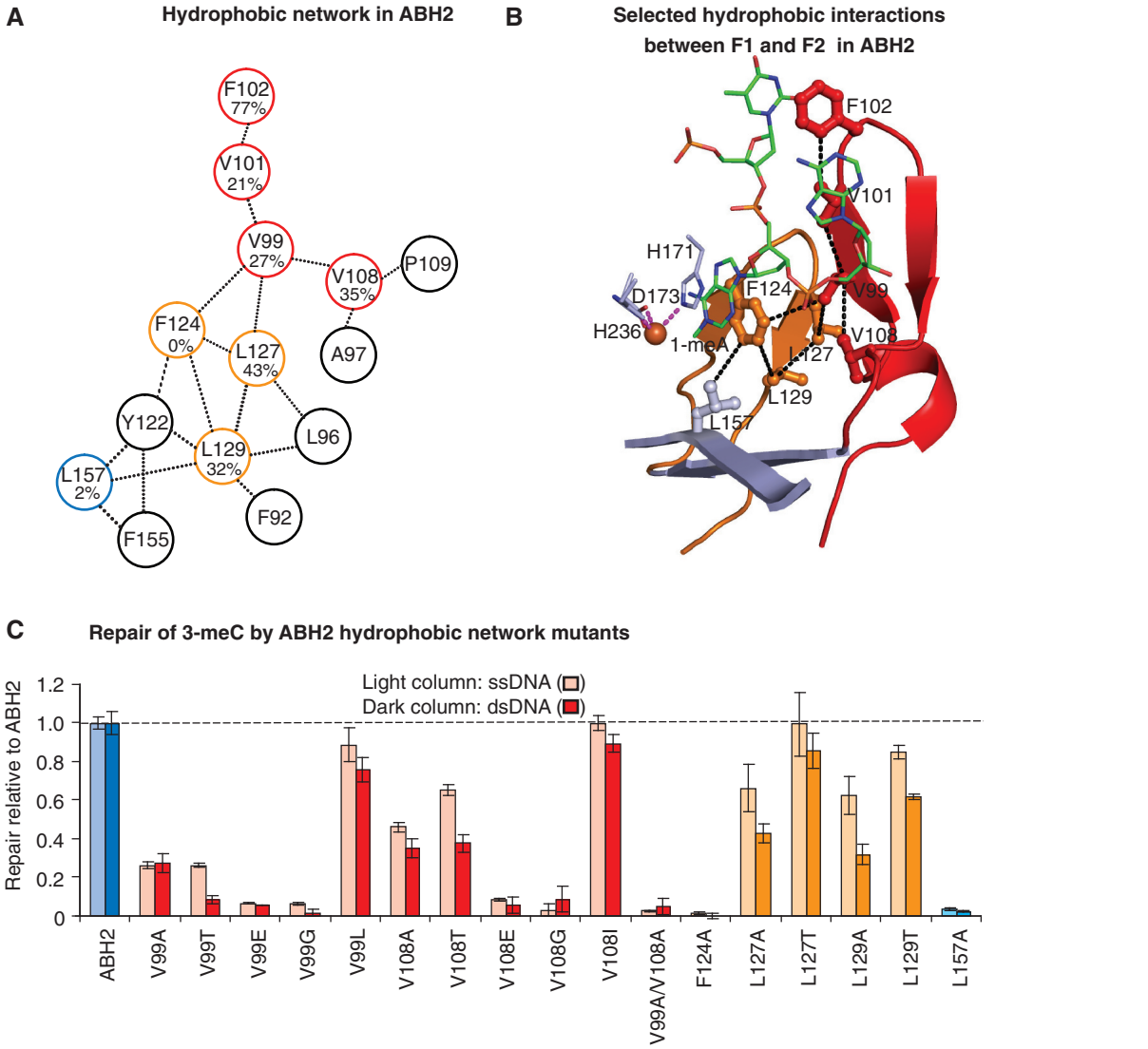

Figure 4. Hydrophobic network in ABH2 required for base flipping and stabilization in the active site. (**A**) Schematic presentation of residues in the hydrophobic network (<5Å, dashed black lines), with residues selected for mutagenesis displayed as red (F1 residues), orange (F2 residues) or blue rings (active site). Activities of Ala variants on dsDNA were compared to wt ABH2 as indicated. (**B**) The hydrophobic network comprises residues in F1 (V99, V101, F102 and V108, in red), in F2 (F124, L127 and L129, in orange) and L157 (light blue) in the β-jelly roll fold. The lesion-containing strand is presented as indicated. The ferrous iron (light brown sphere) is coordinated (dashed magenta lines) by H171, D173 and H236, presented as light-blue lines (PDB ID: 3buc). (**C**) Repair activity of ABH2 hydrophobic network mutants. The 1 pmol substrate was incubated with 1 pmol protein for 20 min at 37°C. Error bars represent standard deviation.

of methyl in the Cγ2 position (in V108) had similar but less pronounced effect, possibly caused by loss of hydrophobic interaction with A97.

The hydrophobic network also comprises the conserved Y122, F124, L127 and L129 in F2 (Figure 4A and B and Supplementary Figure S4). The extra-helical damaged base is sandwiched between H171 in the $HxDx_NH$ motif and F124 (11). The F124A mutant was catalytically dead, presumably mainly because of loss of the important base-stacking function of Phe (Figure 4C). To test if L127 and L129 in the hydrophobic network provided more than shape complementarity to the structure, we replaced them with Ala or Thr. The L127A and L129A mutants displayed similar reduction in activity compared to wtABH2. Interestingly, the reduction was more pronounced with dsDNA than with ssDNA substrates for both Ala variants. The L127T mutant, however, retained wt activity with ssDNA and ~90% activity with dsDNA, suggesting that L127T Cγ2 replaces most of the hydrophobic interactions provided by L127 Cδ1 and Cδ2 atoms. A Thr residue in position 129 also partially compensated for the interactions made by the Cδ atoms of L129.

ABH2-L157 is an active site residue positioned in the catalytic ds β-roll domain, but it is also part of the hydrophobic network (Figure 4A and B). L157 corresponds to the catalytically important L177 in ABH3 and L118 in AlkB (7,9). The ABH3-L177A mutant retained ~30% wt activity when assayed on 3-meC in ssDNA (9), whereas ABH2-L157A only retained 2–3% activity (Figure 4C). Furthermore, site directed mutants of residue L177 in ABH3 (L177A/I/M/N) caused significantly larger loss of demethylation of 1-meA compared with 3-meC. These observations point to a role L177 and L157 in exact positioning of substrate in the active site, possibly serving a role as buffer stop.

The unexpected importance of the hydrophobic residues V99, V101, V108, L127 and L129 in F1 and F2 suggests that these residues must be hydrophobic and provide shape complementarity in the DNA-binding groove of the enzyme–substrate complex for optimal activity. The cooperative function provided by these residues is more important to ABH2 activity in dsDNA than in ssDNA context. As a test for the structural integrity of the ABH2 mutants, we also measured their ability to decarboxylate 2OG. For all eight hydrophobic network mutants examined, decarboxylase activity was better preserved than demethylase activity and with the exception of L157A, decarboxylase activity ranged from 80–120% of wt (Supplementary Figure S5). L157 may be a special case since it is an active-site residue in proximity of 2OG, although not directly interacting. Furthermore, mutants engaged in the proposed hydrophobic network were obtained in fairly similar yields during purification (data not shown). This indicates that their solubility and folding were not substantially deranged.

DISCUSSION

We have explored the molecular basis for the divergent functions of human ABH2 and ABH3. These proteins are closely related members of the AlkB subfamily of dioxygenases that use O_2 and 2OG as co-substrates in oxidative demethylation of DNA or RNA. Structural data have indicated that residues in short, divergent loop motifs may be involved in determining substrate preferences (9–11). Comparisons based on structure and sequence alignments guided us in targeting of potentially important residues by site-directed mutagenesis. Deletion of F1 in ABH2 and ABH3 demonstrates that this motif is essential for the repair of methylated bases, while some capacity for uncoupled decarboxylation of 2OG was retained (Supplementary Figure S3). Swapping the F1 motifs between the enzymes verified that F1 is central in determining substrate preferences (Figure 1). Structure-based alignment of F1 loops of ABH1, ABH2, ABH3 and FTO demonstrated very low overall conservation. However, Val, Lys and Pro residues were found in corresponding positions in three out of the four human AlkB homologues (Supplementary Figure S6).

The elegant structure of ABH2 in complex with a DNA oligonucleotide suggested a prominent role of the side chain of F102 that intercalates the base stack via the minor groove (11). Unexpectedly, site directed mutagenesis of this residue alone (F102A mutant) had little effect on ds and ssDNA repair, while its hydrophobic neighbour, V101, was much more important. However, the double mutant (V101A/F102A) was catalytically dead, demonstrating the functional significance of these hydrophobic residues as a pair (Figure 3). The F102E variant was also inactive. Further bioinformatic analysis and site-directed mutagenesis identified a larger functionally important hydrophobic network unique to ABH2. This network comprises residues in F1, F2 and the active site (Figure 4). A similar hydrophobic network is not present in ABH3. Apparently, ssDNA preference is less exactly tailored than dsDNA repair, both in ABH2 and ABH3. Thus, several of the ABH2 mutants that had lost dsDNA repair capacity retained essentially full ssDNA repair capacity (Figure 3). Furthermore, mutagenesis of ABH3 revealed that charged residues in its F1 β-hairpin have a role in discrimination against use of dsDNA, rather than to promote ssDNA repair. Thus, inserting hydrophobic residues instead of the acidic ones generally did not affect capacity for ssDNA repair significantly, but resulted in gain of dsDNA repair capacity (Figure 2). Importantly, mutants in the hydrophobic network in ABH2 generally affected decarboxylase activity far less than demethylase activity, indicating that the structures of the mutant proteins were not grossly deranged.

In general, DNA repair enzymes may intercalate different types of residues, yet most commonly hydrophobic or positively charged ones, into the DNA helix to flip and stabilize the enzyme–substrate complex. V101 and F102 of ABH2 together are apparently central for catalytic activity by forming a wedge that stacks between bases located both in the lesion and complementary strand. The orphan base is stably flipped out, while the adjacent downstream base is left in a (partly) flipped-out position (11). V101 may also contribute by partially occupying the vacant space from the flipped out deoxyribose. The interacting pair F102/V101 is probably also important by

providing optimal shape complementarity of the intercalating F1 β-hairpin. A similar dual β-hairpin wedge is found in AAG (3-alkyladenine DNA glycosylase), where the wedge is composed of I161 and Y162. However, the Y162A mutant of AAG had minimal glycosylase activity (20), while no data is available for I161.

In addition to stabilizing the hydrophobic network, ABH2-L157 located in close proximity of the active site may function as a buffer stop to position the methylated base for the oxidation reaction. The corresponding residue, L177, in ABH3 is also important for catalytic activity (9), although not to the same degree as ABH2-L157, which may also have an important role in connecting the catalytic domain with the flexible loop segments, F1 and F2, involved in flipping and stabilization of the damaged base in an extra-helical position. ABH3-L177 in the active site is easily autooxidized, presumably inactivating the protein, but a physiological role of this oxidation remains a possibility (9). Thus, a form of AlkB with low-substrate affinity apparently resulted from self-hydroxylation of W178, but oxidation at L118 (L157 in ABH2) was not excluded (21).

Taken together, these findings provide a detailed understanding of how substrate interaction and specificity occurs in the human AlkB homologues ABH2 and ABH3. We show that their divergent F1 motifs and a unique hydrophobic network in ABH2 are involved in substrate preferences. Alignments of the AlkB family of proteins indicate that other AlkB homologues are likely to have similar overall folds (22) and several, if not all, hold distinct motifs corresponding to F1, possibly involved in substrate interaction (9–11,18,23). The wide substrate diversity of 2OG-dependent members of the dioxygenase family is intriguing, given the conserved structure and catalytic mechanism. Among the nine AlkB homologues identified, ABH1, ABH3 (7,18) and FTO (23) share the ability to demethylate ssDNA and RNA *in vitro*, but unlike ABH2 they work very poorly on dsDNA. However, only ABH2 has a well documented function in DNA repair *in vivo*, and ABH3 apparently does not contribute measurably (15). If ABH3 has a role in DNA repair it could be limited to special ssDNA areas. It is possible that F1 and F2 of ABH3 are involved in binding of substrates other than DNA, e.g. RNA. It is not even clear that the major substrate would represent repair of aberrant lesions, since some of the potential RNA substrates (e.g. 3-meC) are also found as normal modifications.

SUPPLEMENTARY DATA

Supplementary Data are available at NAR Online.

FUNDING

Norwegian Cancer Society; The Svanhild; Arne Must Fund for Medical Research and The Research Council of Norway. Funding for open access charge: The Research Council of Norway.

Conflict of interest statement. None declared.

REFERENCES

1. Hecht,S.S. (2008) Progress, challenges in selected areas of tobacco carcinogenesis. *Chem. Res. Toxicol.*, **21**, 160–171.
2. Rydberg,B. and Lindahl,T. (1982) Nonenzymatic methylation of DNA by the intracellular methyl group donor S-adenosyl-L-methionine is a potentially mutagenic reaction. *EMBO J.*, **1**, 211–216.
3. Marchesi,F., Turriziani,M., Tortorelli,G., Avvisati,G., Torino,F. and De Vecchis,L. (2007) Triazene compounds: mechanism of action and related DNA repair systems. *Pharmacol. Res.*, **56**, 275–287.
4. Duncan,T., Trewick,S.C., Koivisto,P., Bates,P.A., Lindahl,T. and Sedgwick,B. (2002) Reversal of DNA alkylation damage by two human dioxygenases. *Proc. Natl Acad. Sci. USA*, **99**, 16660–16665.
5. Falnes,P.O., Johansen,R.F. and Seeberg,E. (2002) AlkB-mediated oxidative demethylation reverses DNA damage in Escherichia coli. *Nature*, **419**, 178–182.
6. Trewick,S.C., Henshaw,T.F., Hausinger,R.P., Lindahl,T. and Sedgwick,B. (2002) Oxidative demethylation by Escherichia coli AlkB directly reverts DNA base damage. *Nature*, **419**, 174–178.
7. Aas,P.A., Otterlei,M., Falnes,P.O., Vågbø,C.B., Skorpen,F., Akbari,M., Sundheim,O., Bjørås,M., Slupphaug,G., Seeberg,E. *et al.* (2003) Human and bacterial oxidative demethylases repair alkylation damage in both RNA and DNA. *Nature*, **421**, 859–863.
8. Hausinger,R.P. (2004) FeII/alpha-ketoglutarate-dependent hydroxylases and related enzymes. *Crit. Rev. Biochem. Mol. Biol.*, **39**, 21–68.
9. Sundheim,O., Vågbø,C.B., Bjørås,M., Sousa,M.M., Talstad,V., Aas,P.A., Drabløs,F., Krokan,H.E., Tainer,J.A. and Slupphaug,G. (2006) Human ABH3 structure and key residues for oxidative demethylation to reverse DNA/RNA damage. *EMBO J.*, **25**, 3389–3397.
10. Yu,B., Edstrom,W.C., Benach,J., Hamuro,Y., Weber,P.C., Gibney,B.R. and Hunt,J.F. (2006) Crystal structures of catalytic complexes of the oxidative DNA/RNA repair enzyme AlkB. *Nature*, **439**, 879–884.
11. Yang,C.-G., Yi,C., Duguid,E.M., Sullivan,C.T., Jian,X., Rice,P.A. and He,C. (2008) Crystal structures of DNA/RNA repair enzymes AlkB and ABH2 bound to dsDNA. *Nature*, **452**, 961–965.
12. Holland,P.J. and Hollis,T. (2010) Structural and mutational analysis of Escherichia coli AlkB provides insight into substrate specificity and DNA damage searching. *PLoS ONE*, **5**, e8680.
13. Sundheim,O., Talstad,V.A., Vågbø,C.B., Slupphaug,G. and Krokan,H.E. (2008) AlkB demethylases flip out in different ways. *DNA Repair*, **7**, 1916–1923.
14. Gilljam,K.M., Feyzi,E., Aas,P.A., Sousa,M.M., Muller,R., Vågbø,C.B., Catterall,T.C., Liabakk,N.B., Slupphaug,G., Drabløs,F. *et al.* (2009) Identification of a novel, widespread, and functionally important PCNA-binding motif. *J. Cell. Biol.*, **186**, 645–654.
15. Ringvoll,J., Nordstrand,L.M., Vågbø,C.B., Talstad,V., Reite,K., Aas,P.A., Lauritzen,K.H., Liabakk,N.B., Bjørk,A., Doughty,R.W. *et al.* (2006) Repair deficient mice reveal mABH2 as the primary oxidative demethylase for repairing 1meA and 3meC lesions in DNA. *EMBO J.*, **25**, 2189–2198.
16. Ougland,R., Zhang,C.M., Liiv,A., Johansen,R.F., Seeberg,E., Hou,Y.M., Remme,J. and Falnes,P.O. (2004) AlkB restores the biological function of mRNA and tRNA inactivated by chemical methylation. *Mol. Cell*, **16**, 107–116.
17. Sarkar,G. and Sommer,S.S. (1990) The "megaprimer" method of site-directed mutagenesis. *Biotechniques*, **8**, 404–407.
18. Westbye,M.P., Feyzi,E., Aas,P.A., Vågbø,C.B., Talstad,V.A., Kavli,B., Hagen,L., Sundheim,O., Akbari,M., Liabakk,N.B. *et al.* (2008) Human AlkB homolog 1 is a mitochondrial protein that demethylates 3-methylcytosine in DNA and RNA. *J. Biol. Chem.*, **283**, 25046–25056.
19. Tina,K.G., Bhadra,R. and Srinivasan,N. (2007) PIC: Protein Interactions Calculator. *Nucleic Acids Res.*, **35**, W473–W476.

20. Lau,A.Y., Wyatt,M.D., Glassner,B.J., Samson,L.D. and Ellenberger,T. (2000) Molecular basis for discriminating between normal and damaged bases by the human alkyladenine glycosylase, AAG. *Proc. Natl Acad. Sci. USA*, **97**, 13573–13578.
21. Bleijlevens,B., Shivarattan,T., Flashman,E., Yang,Y., Simpson,P.J., Koivisto,P., Sedgwick,B., Schofield,C.J. and Matthews,S.J. (2008) Dynamic states of the DNA repair enzyme AlkB regulate product release. *EMBO Rep.*, **9**, 872–877.
22. Kurowski,M.A., Bhagwat,A.S., Papaj,G. and Bujnicki,J.M. (2003) Phylogenomic identification of five new human homologs of the DNA repair enzyme AlkB. *BMC Genomics*, **4**, 48.
23. Gerken,T., Girard,C.A., Tung,Y.C., Webby,C.J., Saudek,V., Hewitson,K.S., Yeo,G.S., McDonough,M.A., Cunliffe,S., McNeill,L.A. *et al*. (2007) The obesity-associated FTO gene encodes a 2-oxoglutarate-dependent nucleic acid demethylase. *Science*, **318**, 1469–1472.